Electronic Supplementary Information

Conjugation of RNA via 2'-OH acylation: Mechanisms determining nucleotide reactivity

Biswarup Jash and Eric T. Kool*,

Department of Chemistry, Stanford University, Stanford, CA 94305, USA

Email: kool@stanford.edu

Contents

1. Materials and Methods

Chemicals

All chemicals were purchased from Sigma Aldrich unless mentioned specifically. The solid-phase oligoribonucleotide syntheses used 2'-TBDMS-protected ribonucleoside (*N*,*N*-diisopropyl)phosphoramidites with A^{Ac} (A^{bz} for 3'-TBDMS-protected) , G^{Ac}, C^{Ac} as protected bases. The phosphoramidates were purchased from ChemGenes (Wilmington, MA). The controlled-pore glass (cpg) loaded with the first nucleoside (pore size 1000 Å, loading 20-30 μmol/g) was obtained from Glen Research. For the 5'-phosphorylation of the RNA oligomer, 2-[2-(4,4'-dimethoxytrityloxy)ethylsulfonyl]ethyl-(2-cyanoethyl)-(*N*,*N*-diisopropyl)phosphoramidite, (chemical phosphorylation reagent) was purchased from Glen Research. 1'-methylglycosides were purchased from TCI, USA. 5'-3'-cyclic AMP and 2'-2'-deoxyadenosine were purchased from Fischer Scientific, USA. The HPLC-grade water for sample preparation was purchased from ThermoFisher USA. Anhydrous DMSO was purchased from ThermoFisher and used without further drying.

Mass spectrometry

MALDI-TOF. The MALDI-TOF mass spectra were recorded on a Bruker Daltonik Microflex MALDI-TOF spectrometer with a N_2 laser, in linear negative mode. A MSP BigAnchor 96 ground steel target was used for MALDI-TOF analysis. For the linear negative mode, a mixture of 0.3 M trihydroxyacetophenone in EtOH and 0.1 M aqueous ammonium citrate (2/1, *v/v*) was used as matrix/comatrix, and always freshly prepared before analysis. The spectral data was analyzed with Flex Analysis, version 3.4 (Bruker).

LC-MS. LC-MS and high-resolution mass spectrometric analysis were performed by Vincent Coates Foundation Mass Spectrometry Laboratory at Stanford University.

NMR spectroscopy

^{1}H- and ^{31}P-NMR spectra were recorded on Varian Mercury 400 MHz NMR spectrometer. ^{1}H-NMR spectra were internally referenced to the residual solvent signal.

HPLC

Reverse-phase HPLC was performed on a SHIMADZU UFLC system, using a SunFire semi-preparative C18-column (250 x 10 mm). The flow rate was maintained throughout at 1.5 mL/min, with detection at λ=260 nm. The buffer used in the HPLC was triethylammonium bicarbonate buffer (50 mM, pH 7) and was prepared in house with triethylamine and dry ice.

2. General Protocols for Synthesis

Solid-Phase Synthesis of Chimeric Dinucleotides (**General Protocol A**). The chimeric dinucleotides were synthesized in the DMT-off mode on an ABI synthesizer, using the commercially available phosphoramidite building blocks. All dinucleotides were prepared on a 1 μmol scale with an extended coupling time. After the completion of the synthesis, the cpg loaded with the dinucleotide was dried in a high vacuum, followed by deprotection from the solid support with aqueous ammonium hydroxide solution overnight at room temperature. The supernatant was separated from cpg-bases, and the remaining solid support was washed with water (2 x 1 mL). The combined solution was subjected to a stream of air onto the surface for 2 h min to remove the excess ammonia added during the deprotection. The solution was then lyophilized to dryness. After that, the solid residue was treated with triethylamine trihydrofluoride (0.2 mL) and kept for 4 h at room temperature. The resulting mixture was quenched with methoxytrimethylsilane (1.5 mL) was added, and the mixture was vortexed for 3 min, which resulted in off-white suspension. After that, the mixture was centrifuged for 5 min at 4000 rpm. The supernatant was discarded and dried in air. Then, the solid was dissolved in 2 mL of water, and lyophilized to dryness. Following this, the compound was desalted with a C18 Sep-Pak Vac cartridge (1 g; Milford, MA, USA), using a NaCl gradient method. In this method, the crude sample was dissolved in 5 M NaCl solution (0.5 mL) and loaded on a pre-equilibrated column (2 mL acetonitrile, followed by 20 mL water). Subsequently, 6 mL of 1 M NaCl was passed through the column, followed by 10 mL of water. Finally, the oligo was eluted with 5 % acetonitrile. The oligo containing fractions were collected together and lyophilized to dryness. After that, the dinucleotide was purified by HPLC using a gradient of acetonitrile in triethylammonium bicarbonate buffer (50 mM, pH 7). Finally, the oligonucleotide was further desalted by NaCl gradient method, as described before. The product was quantified by UV-Vis absorbance at 260 nm. Finally, the purity of the dinucleotide was confirmed by HPLC and characterized by MALDI-TOF mass spectroscopy.

Synthesis of Mononucleotides (General Protocol B)

The following protocol is for 3'-dAMP and is representative.

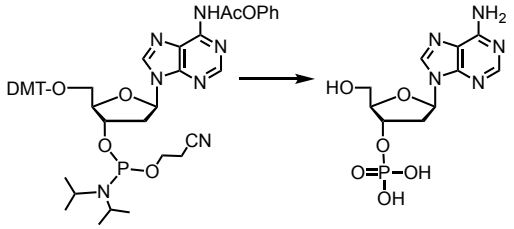

Figure S1. Synthesis of 3'-dAMP from phosphoramidite of solid-phase DNA synthesis.

2'-deoxy 3'-adenosine monophosphate

In a 25 mL round-bottom flask, 5'-dimethoxytrityl-*N*-phenoxyacetyl-2'-deoxyadenosine,3'-[(2-cyanoethyl)-(*N*,*N*-diisopropyl)]-phosphoramidite (100 mg, 0.11 mmol) was dissolved in 2 mL of dry dichloromethane. To it, 1.8 mL of 3% TCA in dichloromethane (Deprotection reagent of DNA synthesizer) was added and stirred for 5 min. To quench the reaction, 3 mL of methanol was added and stirred for another 2 min at room temperature. After that, the solvent was evaporated to dryness under vacuum. To it, 4 mL of oxidizing solution of DNA synthesizer was added and stirred for 15 min. After that, the solvent was evaporated, and the crude product was kept under high vacuum for 30 min. To it, 5 mL of 30 % ammonium hydroxide solution was added and kept overnight in closed condition. Next day, the solution was freed of ammonia by passing a stream of air onto the surface of the solution for 1 hour until the remaining solution was odorless. The solution was then lyophilized to dryness. Afterwards, the crude mixture was purified by RP-HPLC chromatography using 50 mM triethylammonium bicarbonate buffer (TEAB buffer, pH 7) and 0.1% TFA in acetonitrile. The pure fractions were found at 18 % acetonitrile in TEAB buffer. The product containing fractions were collected together, and lyophilized.

The 3'-dAMP was obtained as triethylammonium salt with 1:2 mol ratio and it was converted to sodium salt. For that, it was resuspended in 100 µL of methanol and added to 400 µL of 0.8 M $NaClO_4$ in acetone. The resulting solution was centrifuged at maximum speed for 5 min at 4 °C. The supernatant was discarded, and the obtained white pellet was washed with 400 µL of acetone, followed by centrifugation at 4°C for 5 minutes at max speed. At the end, the pellet was dried in air and resuspended in water. The final yield was determined by UV-Vis spectroscopy.

Yield: 20 % (0.022 mmol).

^{1}H NMR (400 MHz, D_2O) δ= 8.21 (s, 1H), 8.10 (s, 1H), 6.35 (dd, *J* = 7.8, 6.1 Hz, 1H), 4.75 – 4.66 (m, 1H), 4.24 – 4.10 (m, 1H), 3.70 (dd, *J* = 3.7, 2.0 Hz, 2H), 2.71 (dt, *J* = 13.8, 7.0 Hz, 1H), 2.57 (ddd, *J* = 14.0, 6.1, 3.0 Hz, 1H) ppm.

^{31}P NMR (162 MHz, D_2O) δ= 2.45 ppm

ESI-MS: $[M+H]^+$ calculated: 332.1; observed mass: 332.3

TBDMS deprotection for ribonucleotide. The lyophilized sample after ammonia deprotection was treated with 1 mL of the solid was treated with 1 mL of triethylamine trihydrofluoride (1.5 mL, 9.2 mmol) and kept for 4 h at room temperature. Then, 7 mL of methoxytrimethylsilane was added, and the mixture was vortexed for 4 min. To that solution, 1 mL of acetone was added to complete the precipitation. The suspension was centrifuged for 5 min. The supernatant was discarded, and the off-white pellet was washed with 50 mM $NaClO_4$ in acetone. The excess acetone was removed in air. Finally, the off-white precipitate was dissolved in 3 mL of water and subjected to lyophilization. The crude mixture was finally purified by HPLC using a gradient of acetonitrile (containing 0.1% TFA) in triethylammonium bicarbonate buffer (50 mM, pH 7). After salt-exchange the product was quantified by UV-Vis absorbance at 260 nm.

Synthesis of Adenosine 3'-ethylphosphate. The compound was prepared from the commercially available 3'-AMP by following a literature procedure[1, 2]. The desired compound was purified by HPLC using a gradient of acetonitrile (containing 0.1% TFA) in triethylammonium bicarbonate buffer (50 mM, pH 7).

3. Additional Data

Activation of NAI

NAI was prepared as described previously[3]. 2-Methylnicotinic acid and 1,1′-Carbonyldiimidazole were dissolved in dry DMSO in 1:1 ratio in a closed Eppendorf tube. The mixture was kept at room temperature for 1 h, and vortexed thoroughly to remove the dissolved CO_2 from the solution. The resulting solution was used as a stock solution of NAI before during acylation assays. Note that all reactions contain a 1:1 molar mixture of NAI and free imidazole.

Determination of the extinction coefficient of 2-methyl nicotinic acid at 260 nm

Peak areas of NAI adducts measured by HPLC were adjusted for the overlapping absorbance of the nicotinyl adduct. To measure this contribution, an aqueous solution of known concentration of 2-methylnicotinic acid was prepared. The corresponding UV absorbance at 260 nm was recorded for the highest concentration. The solution was diluted successively into varied concentrations and the corresponding absorbance was recorded. Finally, the absorbance was plotted against concentration using the Beer- Lambert equation. The slope of the fit line resulted in the extinction coefficient of the compound at 260 nm. From two independent measurements, the extinction coefficient was found to be 3748 $mol^{-1} \cdot lit \cdot cm^{-1}$.

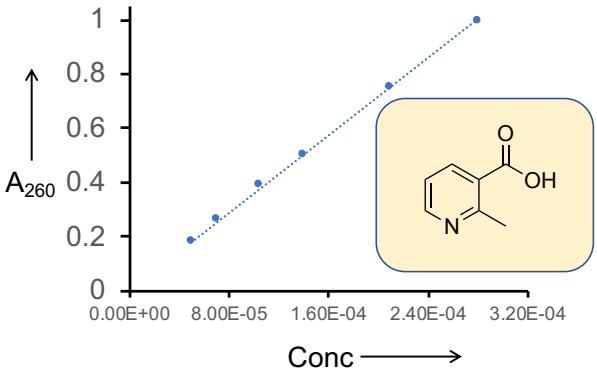

Figure S2. Straight line fitting for the determination of the molar extinction coefficient of 2-methylnicotinic acid at 260 nm.

NMR analysis of hydrolysis rate of NAI acylating agent

In an Eppendorf tube, 2-methylnicotinic acid and 1,1′-carbonyldiimidazole (**CDI**) were mixed in the ratio of 1:1 in dry DMSO-d_6. The resulting mixture was incubated at room temperature for 1 h. In a NMR tube, the resulting NAI was added to a D_2O solution containing 50 mM NaCl and 10 mM MOPS buffer (pH 7). The DMSO content was kept to 5% (*v*/*v*), as followed during acylation assays. The ^{1}H-NMR was recorded at different time intervals. The half-life was calculated by fitting the obtained data to a first-order rate equation (Fig. S4). The half-life was found to be approximately 173 min.

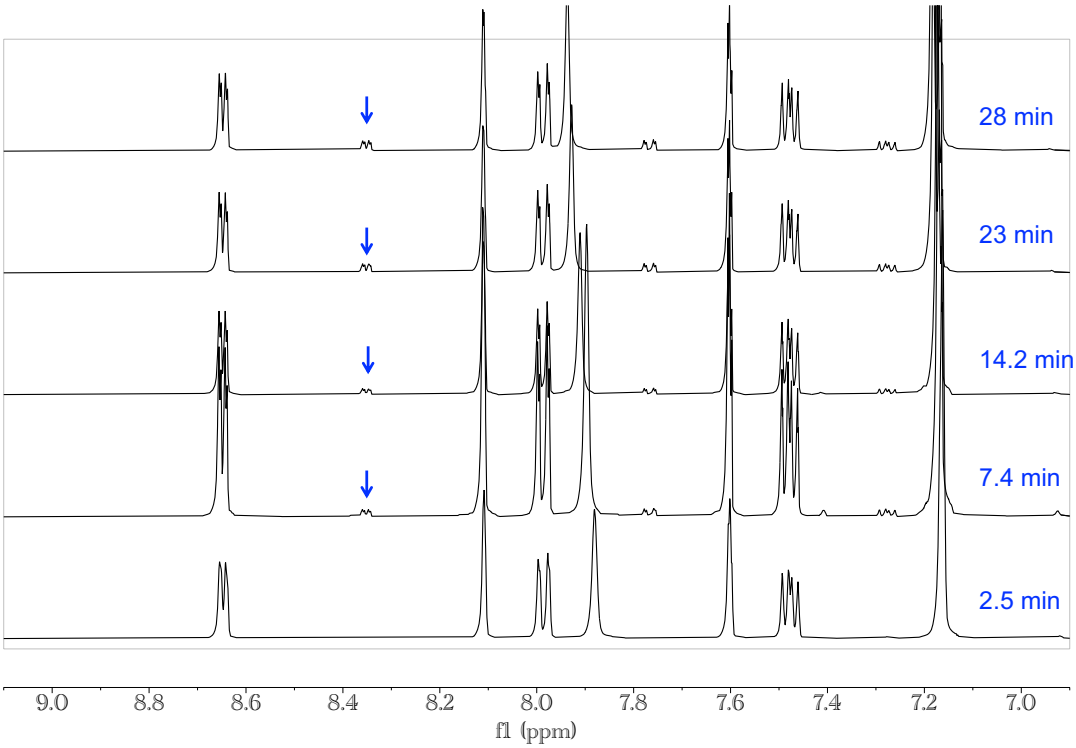

Figure S3. Stacked NMR plots of NAI in D_2O/ DMSO-d_6 (95:5, *v*/*v*). Hydrolysis was monitored with the color-coded peak.

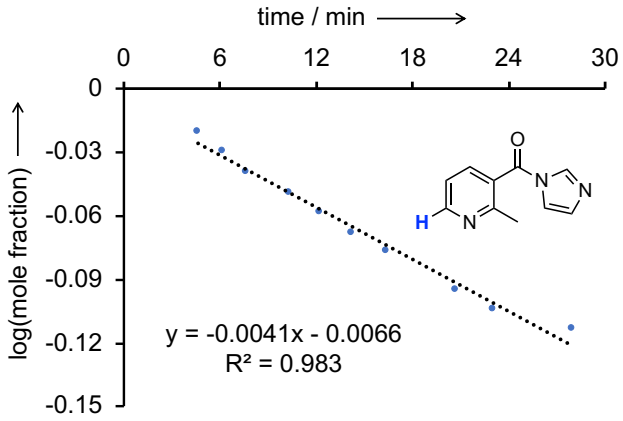

Figure S4. Straight line fit for the determination of half-life of NAI in D_2O/ DMSO-d_6 (95:5 *v*/*v*).

Quenching of NAI

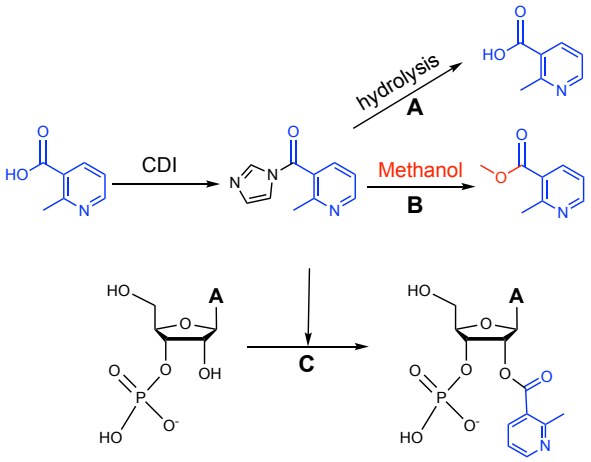

Figure S5. Preparation of NAI, and schematic representation of three different reaction channels during the assay: a) hydrolysis reaction of NAI, b) quenching of NAI by methanol, c) acylation of nucleotides.

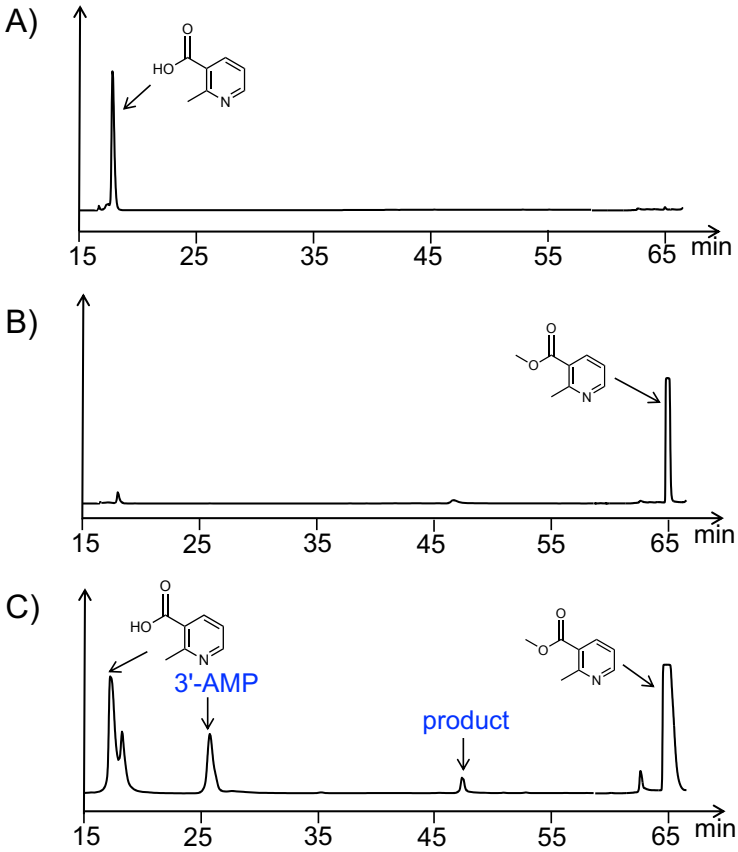

Figure S6. a) HPLC purity profile of pure 2-methyl nicotinic acid; b) HPLC purity profile of pure methyl 2-methylnicotinate; c) HPLC chromatogram from acylation assays involving 3'-AMP with NAI after 9 min reaction time, Conditions: 0.4 mM mononucleotide, 40 mM NAI in DMSO, containing 50 mM NaCl and 10 mM MOPS (pH 7), rt. DMSO content: 5% (*v*/*v*).

Determination of kinetic order of the acylation reaction with adenosine 3'-phosphate

The order of the acylation reaction was determined with respect to 3'-AMP. For that, initial rate was determined by varying the concentration of one of the components while the concentration of the other component was kept constant.

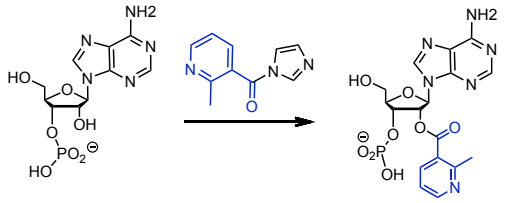

The concentration of 3'-AMP was varied (0.2 mM, 0.4 mM, 0.8 mM) with a single concentration of NAI (40 mM). Similarly, the concentration of NAI was varied (20 mM, 40 mM, 80 mM), while keeping the concentration of 3'-AMP constant at 0.4 mM. In each case, the initial rate of the reaction was determined from HPLC chromatograms. The data points are the average of 2-3 independent reactions. In order to determine the order of the reaction, the logarithm of initial rate was plotted against the logarithm of the concentration of the components, and the slope resulted in the order of the reaction with respect to that particular component.

Kinetic order with respect to 3'-AMP: 0.98 (Figure S7a)

Kinetic order with respect to NAI: 1.1 (Figure S7b)

Overall kinetic order of the reaction is 2.1, confirming a bimolecular mechanism.

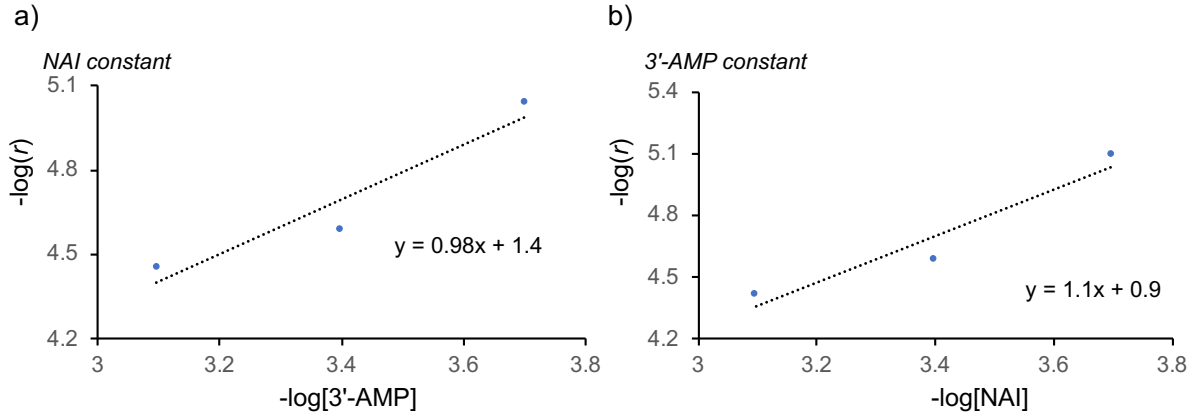

Figure S7. Determination of the kinetic order of the acylation reaction; a) straight line fitting for the determination of the order of 3'-AMP; b) straight line fitting for the determination of the order of NAI. Conditions: 0.2-0.8 mM nucleotide, 20-80 mM NAI, containing 50 mM NaCl and 10 mM MOPS (pH 7), rt. DMSO content: 5% (v/v).

NAI-acylation of 5'-CMP

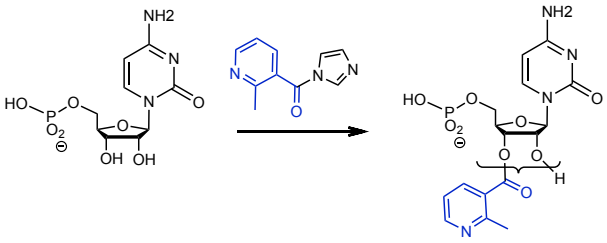

Preparation: At the beginning a 2 M stock solution of NAI in DMSO was prepared (61 mg 2-methyl nicotinic acid and 72 mg CDI). 23 mg of 5'-CMP was dissolved in 0.8 mL of water and used as a stock solution. To a solution containing 50 mM NaCl and 10 mM MOPS (pH 7), 0.8 mL of 5'-CMP stock solution and 0.3 mL of NAI were added. The resulting mixture was incubated at room temperature for 6 h. The crude mixture was concentrated under high vacuum. Finally, the acylated product was purified by HPLC using a gradient of acetonitrile (containing 0.1% TFA) in triethylammonium bicarbonate buffer (50 mM, pH 7).

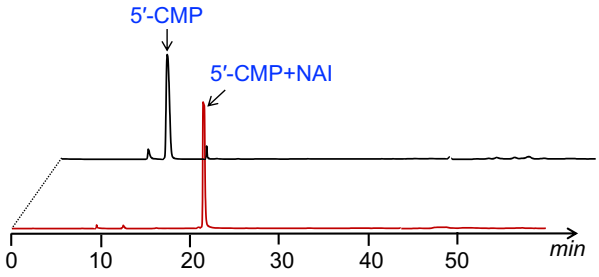

Figure S8. HPLC purity profile of NAI-acylated 5'-CMP.

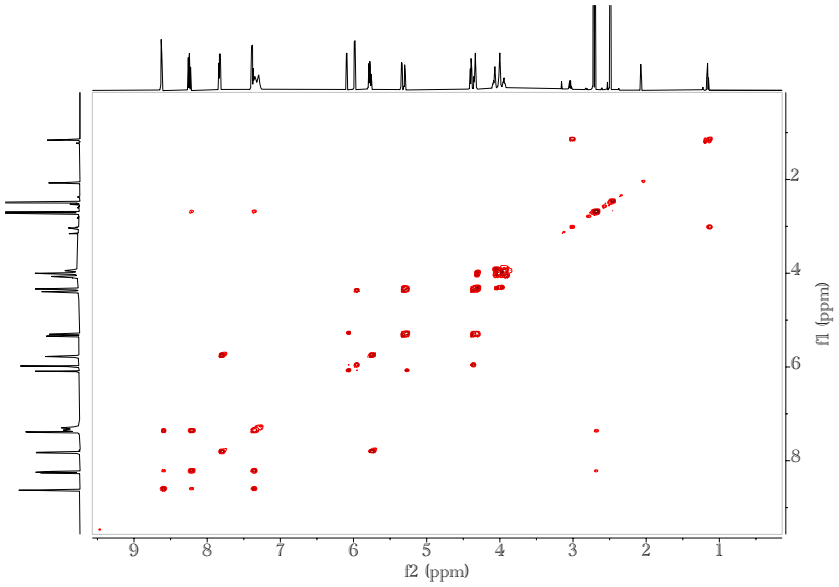

Figure S9. COSY spectrum of NAI-acylated 5'-CMP (400 MHz, DMSO-d6, 298 K).

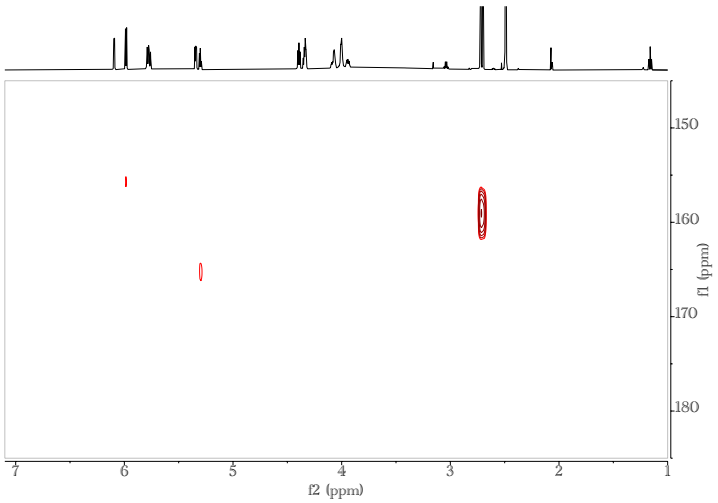

Figure S10. $^{1}H,^{13}C$-HMBC spectrum of NAI-acylated 5'-CMP (400 MHz, DMSO-d6, 298 K). This spectrum confirms the formation of the ester bond.

4. Data of Acylation Kinetics

Acylation of mono- and dinucleotides

Stock solutions of the mononucleotides/dinucleotides were prepared in HPLC-grade water (DNAse and RNAse free), and concentrations were determined by UV absorbance (Nanodrop from Thermo Scientific). To maintain the pH of the solution, MOPS (pH 7) and MES (pH 6) buffer was used during sample preparation. Aliquots of stock solutions of the mononucleotide, buffer and NaCl were added to an Eppendorf tube, followed by the addition of activated NAI to result in final concentration of 0.4 mM of nucleotide, 10 mM buffer, 50 mM NaCl and 40 mM NAI. The final volume was 200 µL while measuring the initial rate of the acylation. The DMSO content was kept to 5% in all assays reported here.

During the assays, 186 µL samples of the reaction mixture were drawn, mixed with 75 µL of methanol for quenching. We monitored the progress of the acylation of the mononucleotide to the acylated mononucleotide. From the HPLC chromatogram, the area under the respective peaks at 260 nm were taken. In addition, the contribution from the NAI chromophore was taken into consideration while determining the yield of the acylation assay. Initial rates were employed to avoid kinetic contributions of the hydrolysis of the acylating agent; pseudo-first-order behavior was observed, keeping yields below 10 % for analysis. For the initial rate determination (the conversion to the product with time**)**, the reaction mixture was quenched at early stages (25 sec-55 sec) by addition of methanol (75 µL for mononucleotide assays, 100 µL for dinucleotide assays) and the mixture was injected to HPLC.

For HPLC analysis, a gradient of acetonitrile (containing 0.1% TFA) in triethylammonium bicarbonate buffer (50 mM, pH 7) was used as solvent system with a flow rate of 1.5 mL/min.

Assays of Mononucleotides

Reference measurements

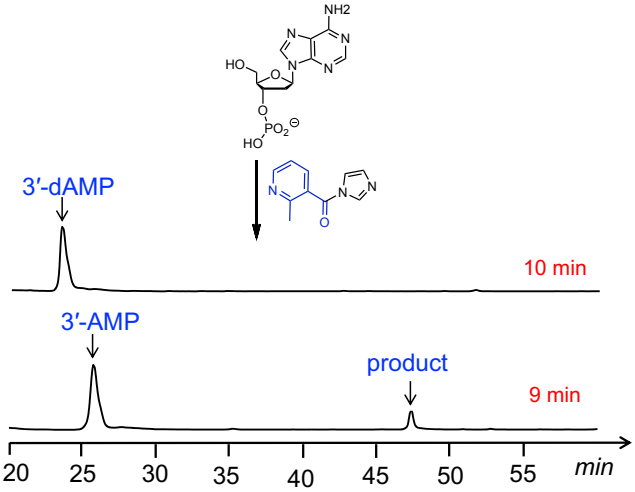

Figure S11. HPLC chromatogram from acylation assays involving **3'-dAMP** and **3'-AMP** with **NAI**, showing lack of reaction with the deoxyribonucleotide. Conditions: 0.4 mM mononucleotide, 40 mM NAI in DMSO, containing 50 mM NaCl and 10 mM MOPS (pH 7), rt. DMSO content: 5% (*v*/*v*).

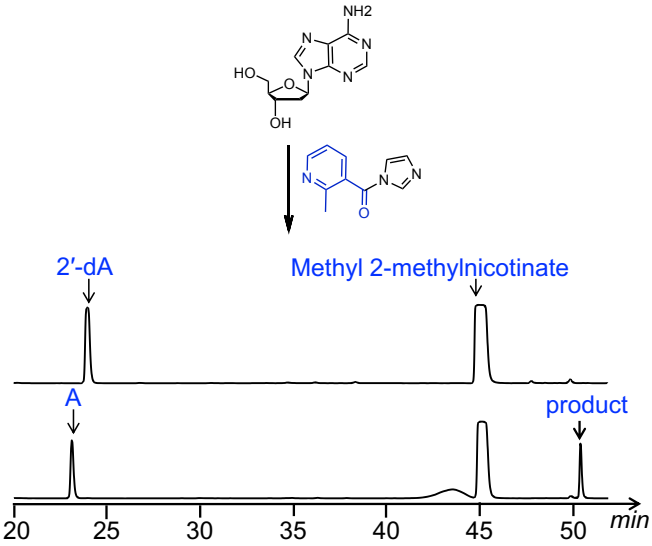

Figure S12. HPLC chromatogram from acylation assays involving **2'-dA** and **A**, with **NAI** after 5 min reaction time. Conditions: 0.4 mM nucleoside, 40 mM NAI in DMSO, containing 50 mM NaCl and 10 mM MOPS (pH 7), rt. DMSO content: 5% (*v*/*v*).

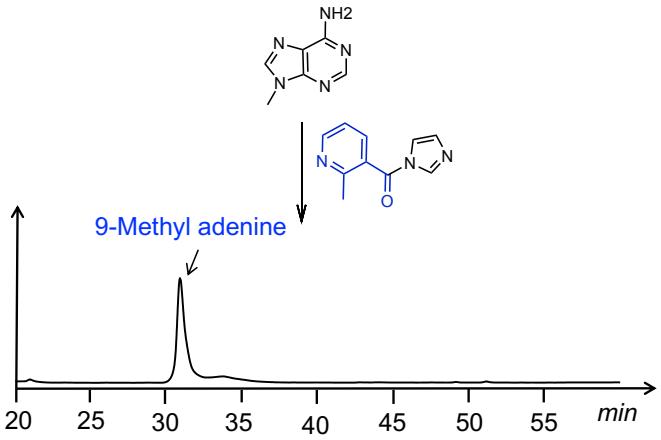

Figure S13. HPLC chromatogram from acylation assays involving 9-methyl adenine and **NAI** after 10 min reaction time, showing no measurable reaction with the exocyclic amine group. Conditions: 0.4 mM nucleobase, 40 mM NAI in DMSO, containing 50 mM NaCl and 10 mM MOPS (pH 7), rt. DMSO content: 5% (*v*/*v*).

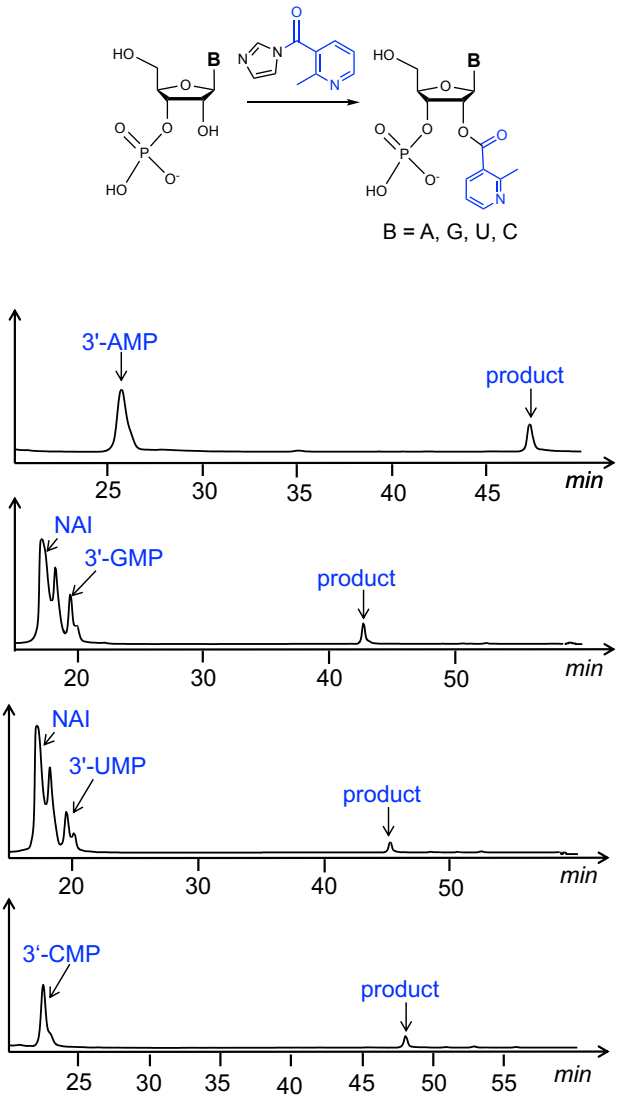

Figure S14. HPLC chromatogram from acylation assays involving the four canonical mononucleotides and NAI after 20 min reaction time, showing single adducts as the chief products. Conditions: 0.4 mM mononucleotide, 40 mM NAI/CDI in DMSO, containing 50 mM NaCl and 10 mM MOPS (pH 7), rt. DMSO content: 5% (*v*/*v*).

Table S1. Conversion (%) observed for ester bond-forming reactions involving mononucleotide and NAI after 20 min reaction time.[a,b]

Entry	Compound	Conversion (%)
1	3'-AMP	16
2	3'-GMP	13
3	3'-UMP	9
4	3'-CMP	8

[a] Yields are determined based on the area under the curve of the signals of interest in the chromatogram.
[b] Conditions: 0.4 mM nucleotide, 40 mM NAI in DMSO, containing 50 mM NaCl and 10 mM MOPS buffer (pH 7), rt. DMSO content**:** 5% (*v*/*v*).

Role of phosphate

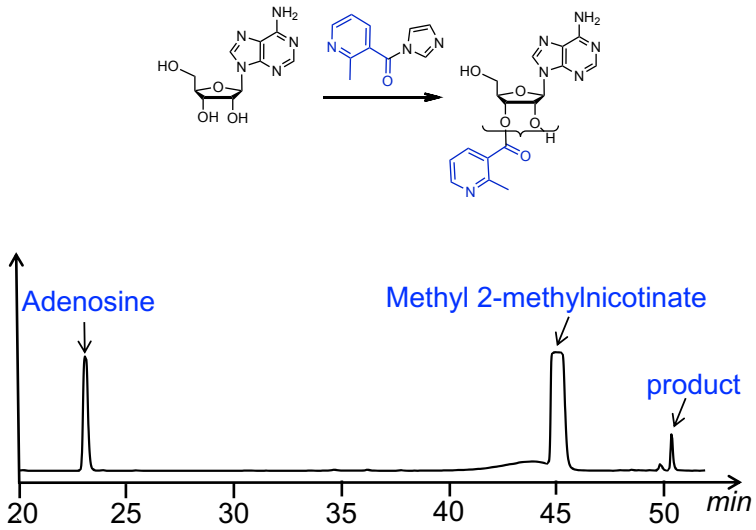

Figure S15. HPLC chromatogram from acylation assays involving reaction of **A** with **NAI** after 40 sec reaction time. Conditions: 0.4 mM dinucleotide, 40 mM NAI in DMSO, containing 50 mM NaCl and 10 mM MOPS (pH 7), rt. DMSO content: 5% (*v*/*v*).

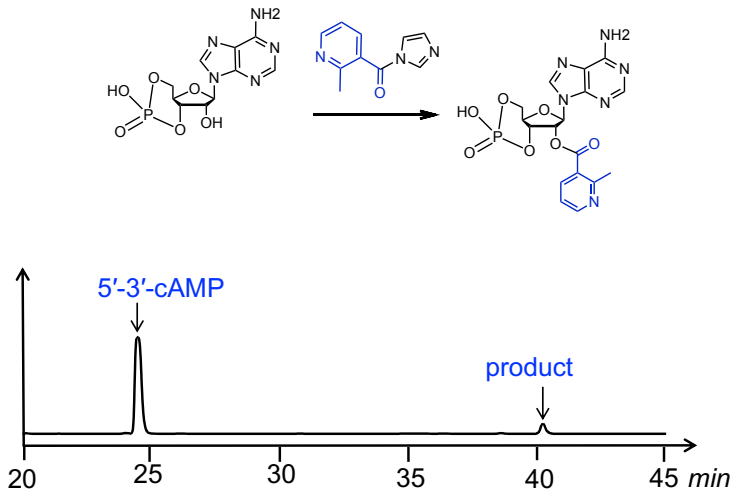

Figure S16. HPLC chromatogram from acylation assays involving reaction of **5'-3'-cAMP** and **NAI** after 40 sec reaction time. Conditions: 0.4 mM mononucleotide, 40 mM NAI in DMSO, containing 50 mM NaCl and 10 mM MOPS (pH 7), rt. DMSO content: 5% (*v*/*v*).

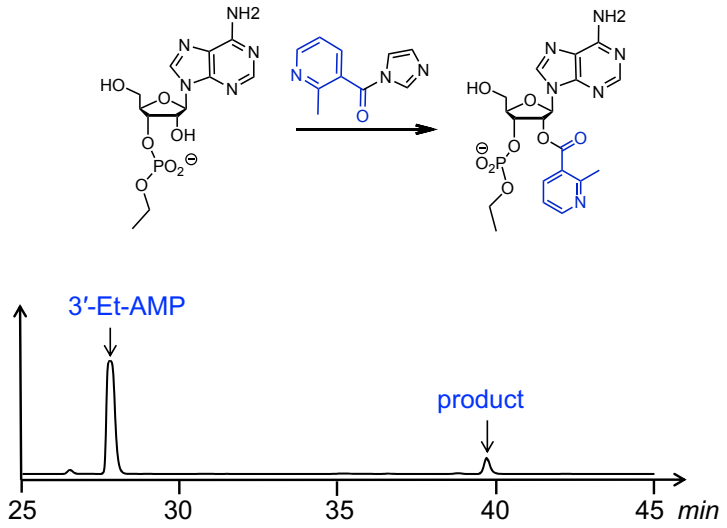

Figure S17. HPLC chromatogram from acylation assays involving 3'-Et-AMP and NAI after 41 sec reaction time. Conditions: 0.4 mM mononucleotide, 40 mM NAI in DMSO, containing 50 mM NaCl and 10 mM MOPS (pH 7), rt. DMSO content: 5% (*v*/*v*).

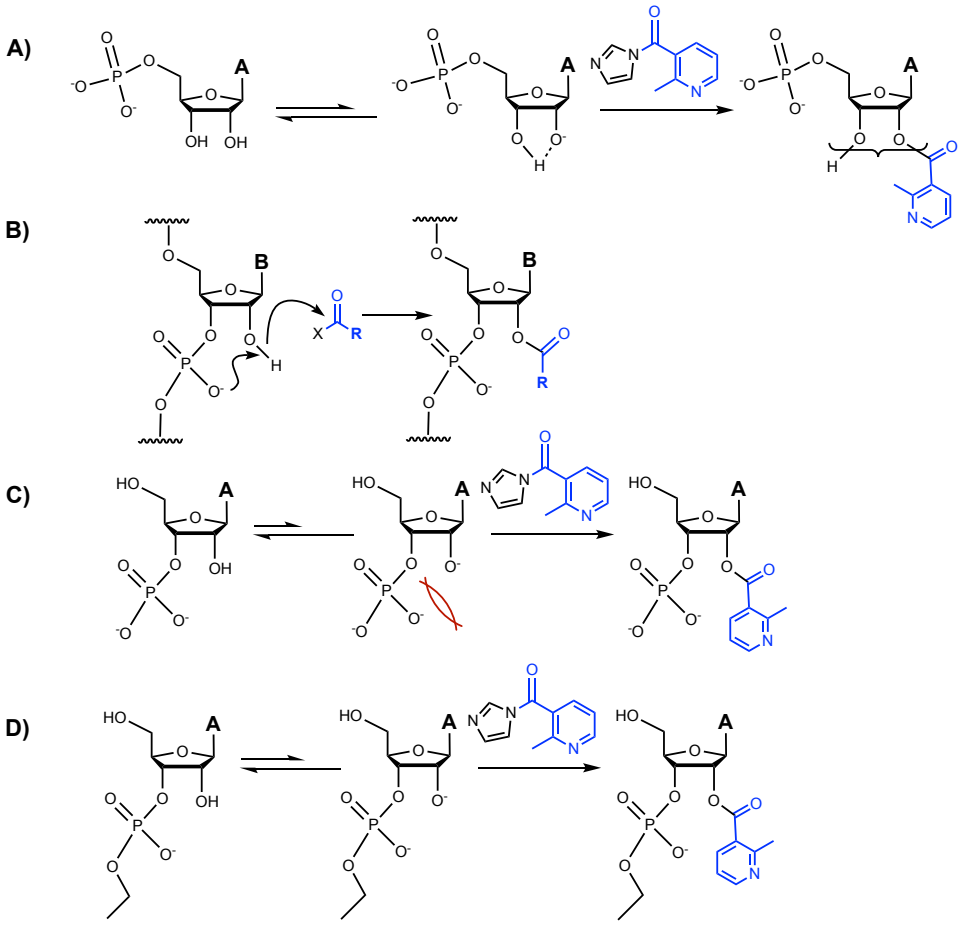

Figure S18. Hypothesized effects of local substitution on 2'-OH acylation of the oxyanion. A) H-bonding by adjacent hydroxyl stabilizes oxyanion (note this can be operative only in mononucleotides and not in RNA); B) Possible general base catalysis by phosphate monoester[4] (not supported by the data); C), D) Hypothesized charge or steric repulsion by neighboring phosphate.

Table S2. Role of phosphate (relative to the 2'-OH) on the kinetics of ester bond-forming reactions. [a,b]

Entry	Compound	k_2 ($mol^{-1} \cdot L \cdot min^{-1}$)
1	**A**	4.67 ± 0.16
2	**5'-AMP**	4.63 ± 0.38
3	**3'-AMP**	1.62 ± 0.04
4	**3'-Et-AMP**	2.37 ± 0.39
5	**5'-3'-cAMP**	2.51 ± 0.18

[a]Yields are determined based on the area under the curve of the signals of interest in the chromatogram.
[b]Conditions: 0.4 mM nucleotide, 40 mM NAI in DMSO, containing 50 mM NaCl and 10 mM MOPS (pH 7), rt. DMSO content**:** 5% (*v*/*v*).
[c]Mean and standard deviation from three independent experiments.

Inductive effects

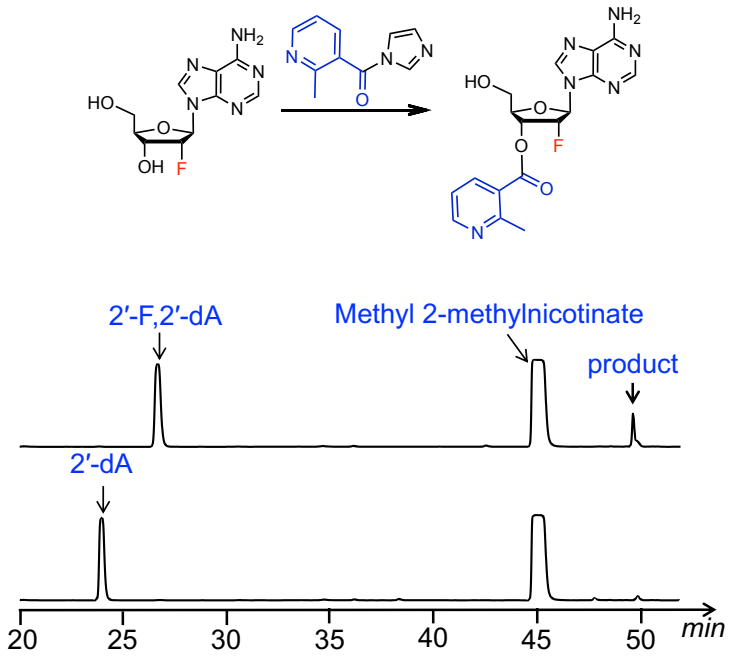

Figure S19. HPLC chromatogram from acylation assays involving nucleosides and NAI after 5min reaction time. Conditions: 0.4 mM mononucleotide, 40 mM NAI in DMSO, containing 50 mM NaCl and 10 mM MOPS (pH 7), rt. DMSO content: 5% (*v*/*v*).

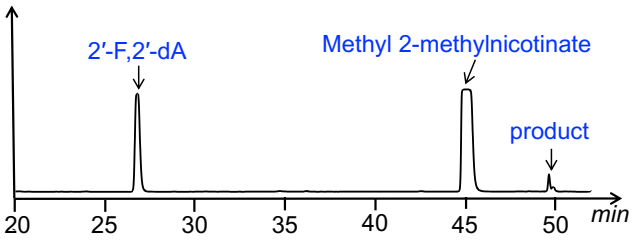

Figure S20. HPLC chromatogram from acylation assays involving 2'-F-2'-dA and NAI after 55 sec reaction time. Conditions: 0.4 mM mononucleotide, 40 mM NAI in DMSO, containing 50 mM NaCl and 10 mM MOPS (pH 7), rt. DMSO content: 5% (*v*/*v*).

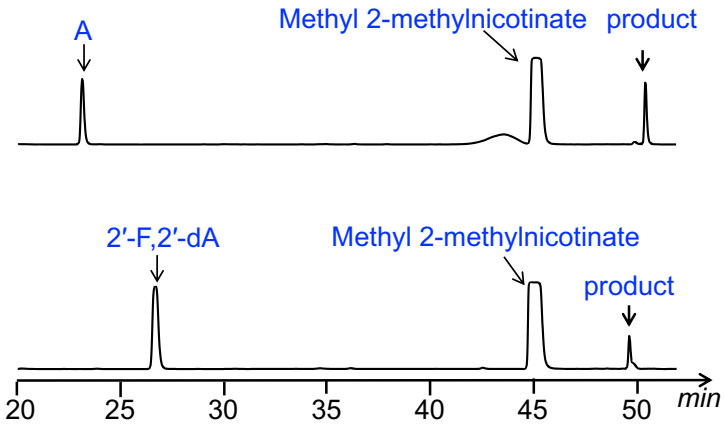

Figure S21. HPLC chromatogram from acylation assays involving nucleosides and NAI after 5min reaction time. Conditions: 0.4 mM mononucleotide, 40 mM NAI in DMSO, containing 50 mM NaCl and 10 mM MOPS (pH 7), rt. DMSO content: 5% (*v*/*v*).

Table S3. Conversion (%) observed for ester bond-forming reactions involving nucleoside and NAI after 5 min reaction time.[a,b]

Entry	Compound	Conversion[c] (%)
1	**2'-dA**	n.d.*
2	**A**	39
3	**2'-F-2'-dA**	12

[a]Yields are determined based on the area under the curve of the signals of interest in the chromatogram.
[b]Conditions: 0.4 mM nucleoside, 40 mM NAI in DMSO, containing 50 mM NaCl and 10 mM MOPS (pH 7), rt. DMSO content**:** 5% (*v*/*v*).
[c]Average of two independent experiments.
*n.d.= not detected

pH effect on the kinetics of acylation

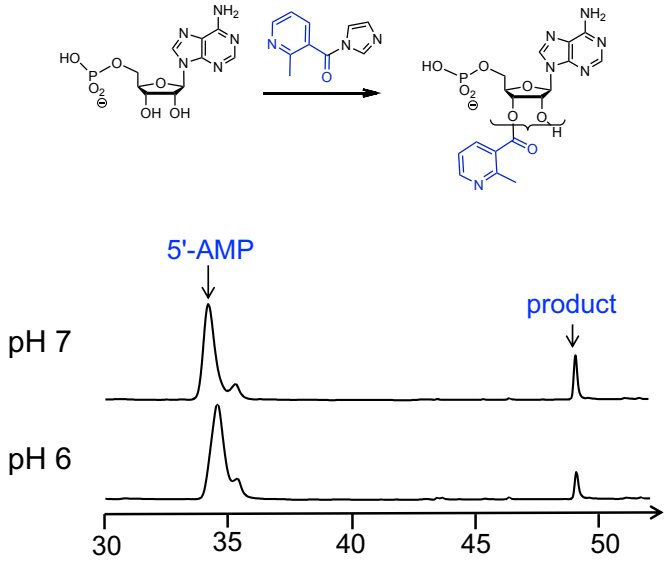

Figure S22. HPLC chromatogram from acylation assays involving **5'-AMP** and **NAI** at two pH values (pH 7, 30 sec; pH 6, 37 sec). Conditions: 0.4 mM nucleotide, 40 mM NAI in DMSO, containing 50 mM NaCl and 10 mM buffer (MOPS for pH 7, MES for pH 6), rt. DMSO content: 5% (*v*/*v*).

Table S4. Effect of pH of the medium on the initial rate of ester bond-forming reactions involving 5'-AMP and NAI, as obtained from the conversion to the product with time [a,b]

Entry	pH	Initial rate (10^{-5} M•min^{-1})
1	7	7.41 ± 0.61
2	6	4.09 ± 0.12

[a]Yields are determined based on the area under the curve of the signals of interest in the chromatogram. [b]Conditions: 0.4 mM mononucleotide, 40 mM NAI in DMSO, containing 50 mM NaCl and 10 mM buffer (MOPS for pH 7, MES for pH 6), rt. DMSO content: 5% (v/v). [c]Mean and standard deviation from three independent experiments.

Acylation of sugar analogues

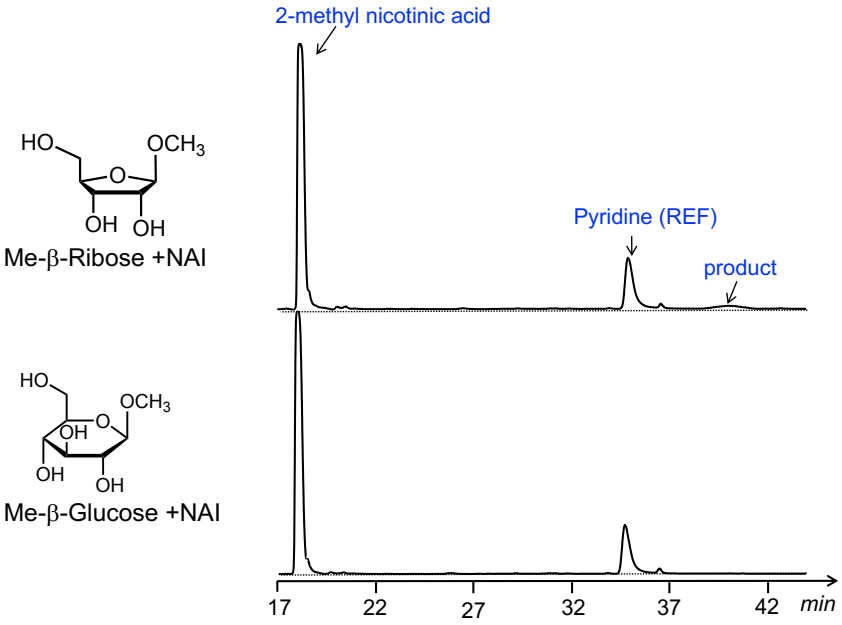

Figure S23. HPLC chromatogram from acylation assays involving 1'-methylglycosides and NAI after 10 min reaction time. Conditions: 0.4 mM sugar, 40 mM NAI in DMSO, containing 50 mM NaCl and 10 mM MOPS (pH 7), rt. DMSO content: 5% (*v*/*v*). After 10 min, equimolar amount of pyridine (0.4 mM) was added to the reaction mixture. The signal of pyridine was used as a reference to determine the conversion.

Table S5. Conversion (%) observed for ester bond-forming reactions involving 1'-methylglycosides and NAI after 10 min reaction time.[a,b]

Entry	Compound	Conversion[c] (%)
1	Me-β-Ribose	18
2	Me-β-Glucose	n.d.*

[a]Yields are determined based on the area under the curve of the signals of interest in the chromatogram, employing the molar absorptivity of NAI. After 10 min, equimolar amount of pyridine was added to the reaction mixture. The signal of pyridine was used as a reference to determine the conversion.
[b]Conditions: 0.4 mM sugar, 40 mM NAI in DMSO, containing 50 mM NaCl and 10 mM MOPS (pH 7), rt. DMSO content**:** 5% (*v*/*v*).
[c]Average of two independent experiments.
*n.d.= no product detected

Discussion of the role of oxyanion formation during the course of acylation

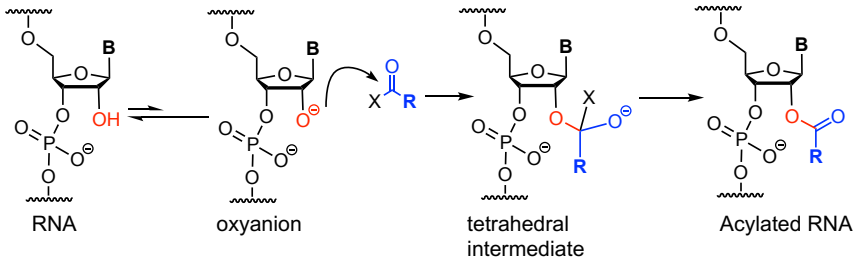

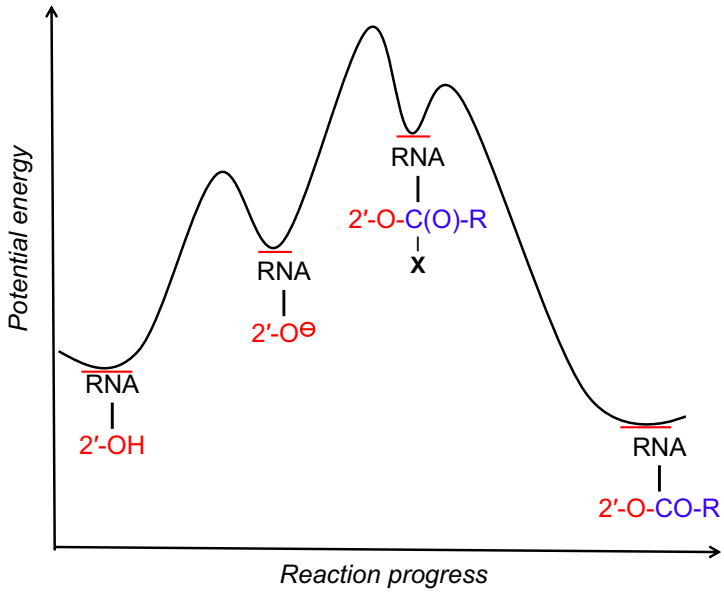

Figure 24. A qualitative potential energy diagram accounting for the hypothesized mechanism of the RNA acylation reaction at 2'-OH based on the experimental observations in the current study. A rapid pre-equilibrium forms the reactive oxyanion (deprotonated by buffer), which is much more reactive than the protonated hydroxyl. This is trapped by the acylimidazole reagent (forming the tetrahedral intermediate) in the rate-limiting step. See discussion below.

The following observations from our study, and previous work, support this mechanism:

(1) The rate is first order in both nucleotide and in acylimidazole. (Note that this is consistent with either protonated or unprotonated hydroxyl as the reacting species)

(2) The secondary 2'-OH reacts faster than the primary 5'-OH in mononucleotides and mononucleosides. This is the opposite of what would be expected if protonated hydroxyl were the reactive species.

(3) Inductive effects from electronegative atoms near the reactive hydroxyl (here 2'-OH) accelerate the reaction. These groups stabilize oxyanion formation, increasing its population in the pre-equilibrium. This is in contrast to what would be expected if the protonated hydroxyl were the reactive species; such electronegative effects would decrease rate by removing electron density from the hydroxyl oxygen, the opposite of what is observed.

(4) Increasing pH speeds reaction. This is consistent with the reaction proceeding via the oxyanion, as higher pH increases the population of this anion. If the protonated hydroxyl were the nucleophile, a change in pH from 6 to 7 would have no effect on rate.

(5) The concept of a rapid pre-equilibrium to form a higher-energy (and more reactive) species in low concentration, through which essentially all of the reaction proceeds, is a well-established principle[5]. Similar effects have been reported previously for reaction of alcohols with acylimidazole reagents, where catalytic amounts of base greatly speed reaction[6, 7].

We note that is also reasonable to consider a general base mechanism, involving deprotonation (likely by water) at the transition state of attack of the 2'-OH on the acyl species. Although we cannot yet rule this out, we currently favor the above pre-equilibrium mechanism, for two reasons: first, inductive effects on the 2'-oxygen make it a very poor nucleophile, and water is a very poor general base at pH=7.

Assays with NAI and Dinucleotides

Reference measurements

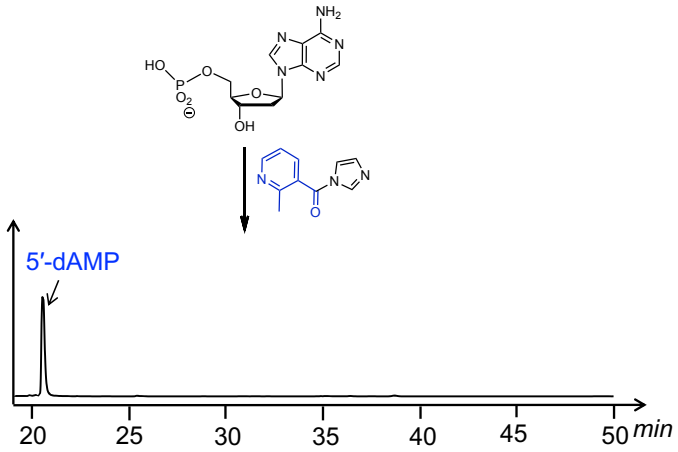

Figure S25. HPLC chromatogram from acylation assays involving **5'-dAMP** with **NAI** after 5 min reaction time. Conditions: 0.4 mM mononucleotide, 40 mM NAI in DMSO, containing 50 mM NaCl and 10 mM MOPS (pH 7), rt. DMSO content: 5% (*v*/*v*).

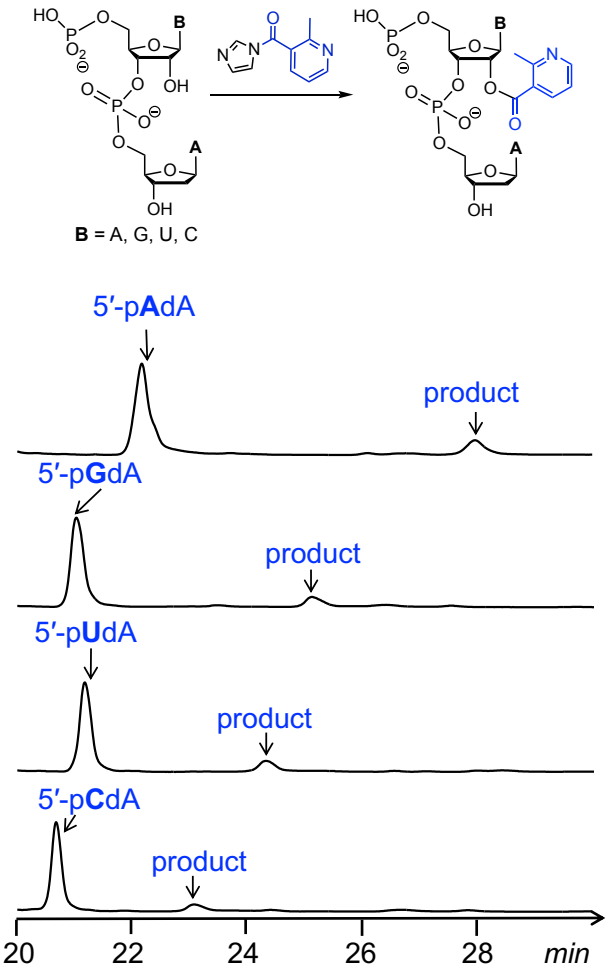

Figure S26. HPLC chromatogram from acylation assays involving dinucleotides and **NAI** after 20 min reaction time. Conditions: 30 µM dinucleotide, 100 mM NAI in DMSO, containing 50 mM NaCl and 10 mM MOPS (pH 7), rt. DMSO content: 5% (*v*/*v*).

Table S6. Conversion (%) observed for ester bond-forming reactions involving dinucleotide and NAI after 20 min reaction time.[a,b]

Entry	Compound	Conversion (%)
1	5'-p**A**pdA	14
2	5'-p**G**pdA	11
3	5'-p**U**pdA	11
4	5'-p**C**dA	10

[a] Yields are determined based on the area under the curve of the signals of interest in the chromatogram.
[b] Conditions: 30 µM dinucleotide, 100 mM NAI in DMSO, containing 50 mM NaCl and 10 mM MOPS (pH 7), rt. DMSO content: 5% (*v*/*v*).

Effect of nucleobase identity on the kinetics of acylation in dinucleotides

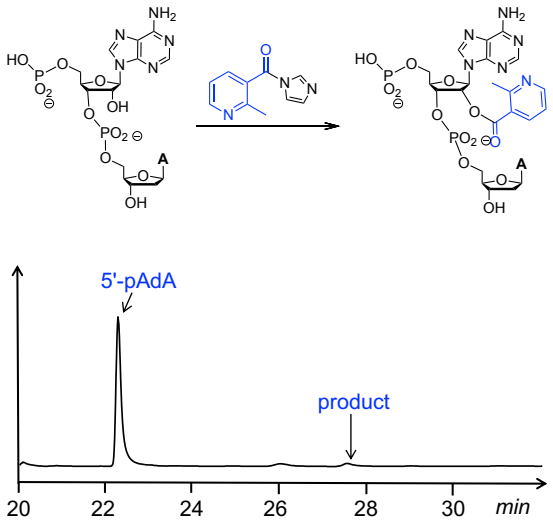

Figure S27. HPLC chromatogram from acylation assays involving 5'-pApdA and NAI after 50 sec reaction time. Conditions: 30 µM dinucleotide, 100 mM NAI in DMSO, containing 50 mM NaCl and 10 mM MOPS (pH 7), rt. DMSO content: 5% (*v*/*v*).

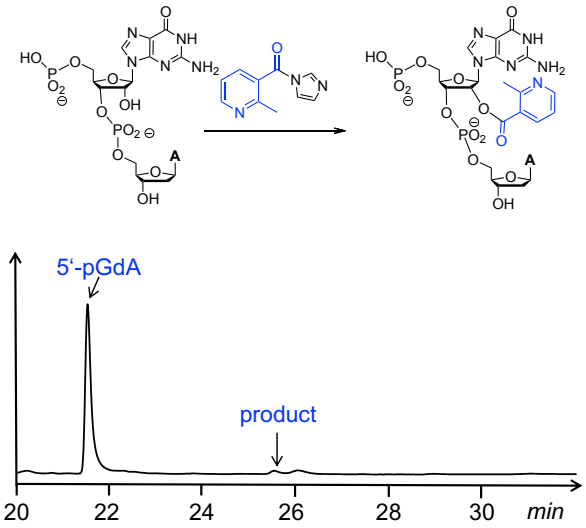

Figure S28. HPLC chromatogram from acylation assays involving 5'-pGpdA and NAI after 55 sec reaction time. Conditions: 30 µM dinucleotide, 100 mM NAI in DMSO, containing 50 mM NaCl and 10 mM MOPS (pH 7), rt. DMSO content: 5% (*v*/*v*).

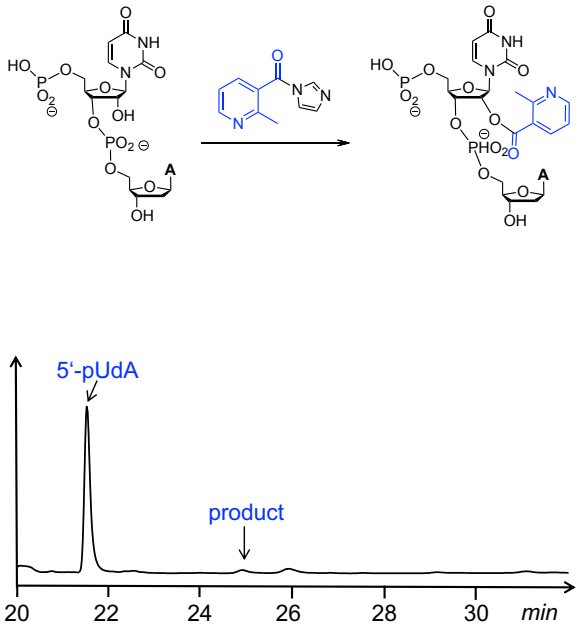

Figure S29. HPLC chromatogram from acylation assays involving 5'-pUpdA and NAI after 50 sec reaction time. Conditions: 30 µM dinucleotide, 100 mM NAI in DMSO, containing 50 mM NaCl and 10 mM MOPS (pH 7), rt. DMSO content: 5% (*v*/*v*).

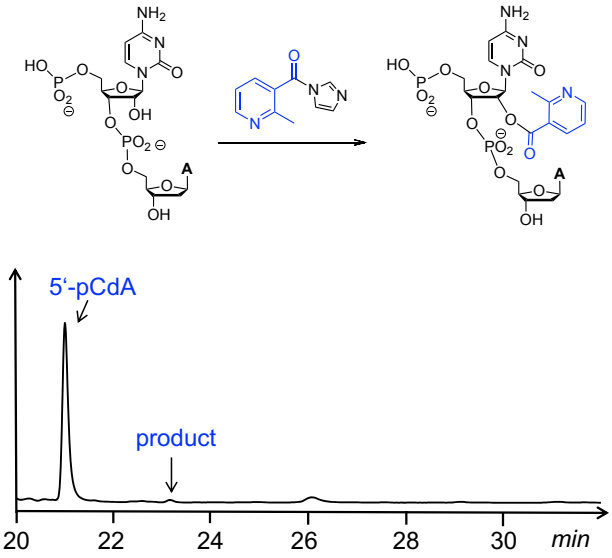

Figure S30. HPLC chromatogram from acylation assays involving 5'-pCpdA and NAI after 50 sec reaction time. Conditions: 30 µM dinucleotide, 100 mM NAI in DMSO, containing 50 mM NaCl and 10 mM MOPS (pH 7), rt. DMSO content: 5% (*v*/*v*).

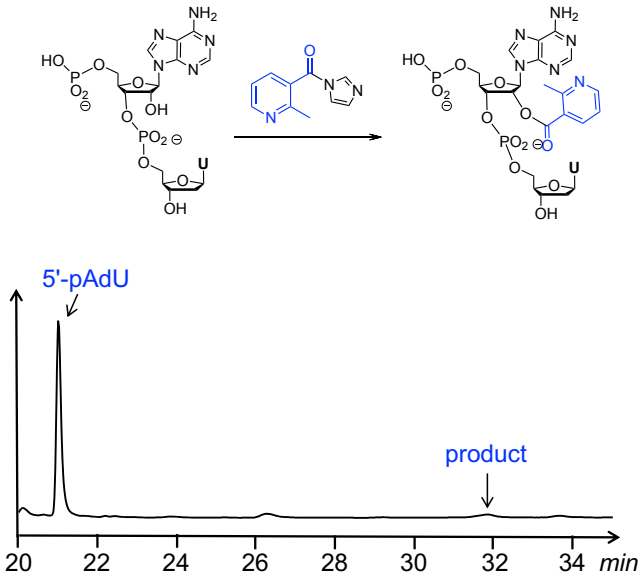

Figure S31. HPLC chromatogram from acylation assays involving 5'-pApdU and NAI after 50 sec reaction time. Conditions: 30 µM dinucleotide, 100 mM NAI in DMSO, containing 50 mM NaCl and 10 mM MOPS (pH 7), rt. DMSO content: 5% (*v*/*v*).

5. Data for Compound Characterisation

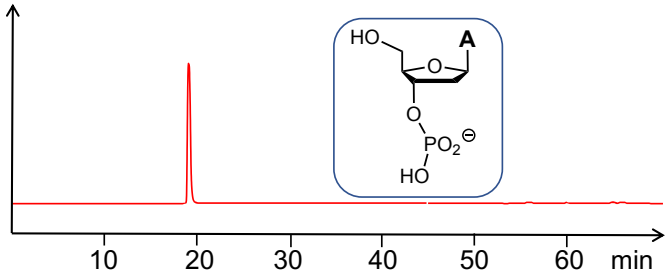

Figure S32. HPLC purity profile of mononucleotide 3'-dAMP.

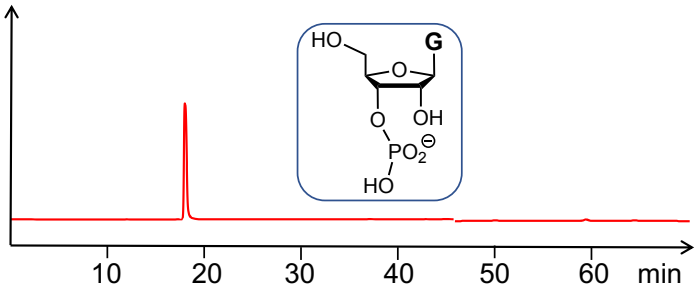

Figure S33. HPLC purity profile of mononucleotide 3'-GMP.

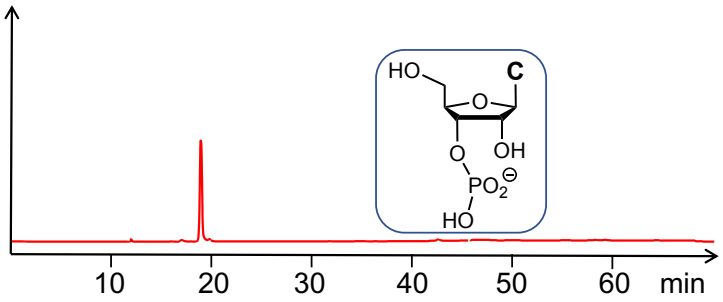

Figure S34. HPLC purity profile of mononucleotide 3'-CMP.

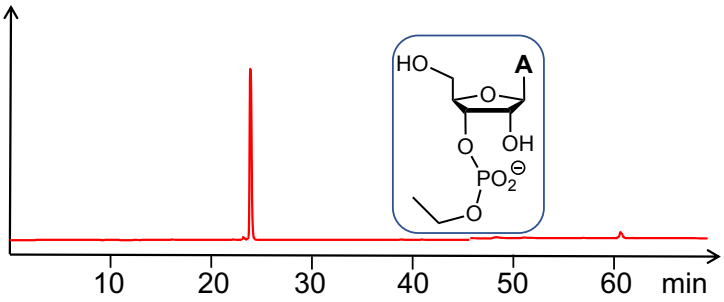

Figure S35. HPLC purity profile of ethyl diester 3'-Et-AMP.

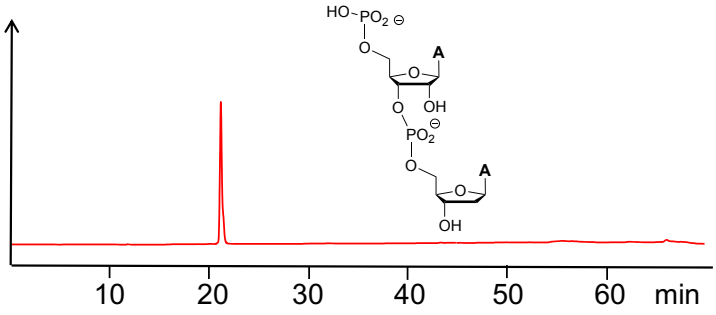

Figure S36. HPLC purity profile of chimeric dinucleotide 5'-pApdA.

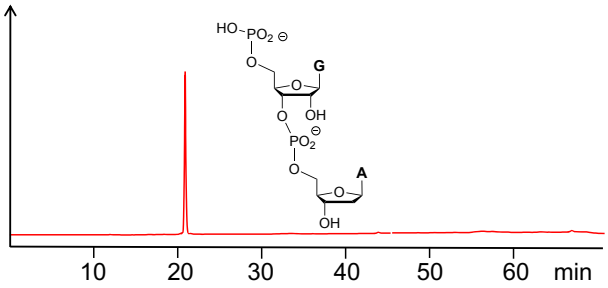

Figure S37. HPLC purity profile of chimeric dinucleotide 5'-pGpdA.

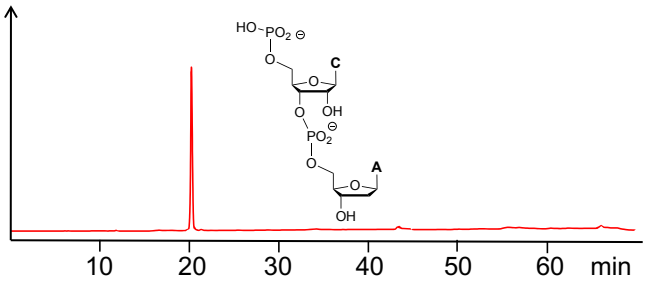

Figure S38. HPLC purity profile of chimeric dinucleotide 5'-pCpdA.

MALDI-TOF Mass Spectra of Chimeric Dinucleotides

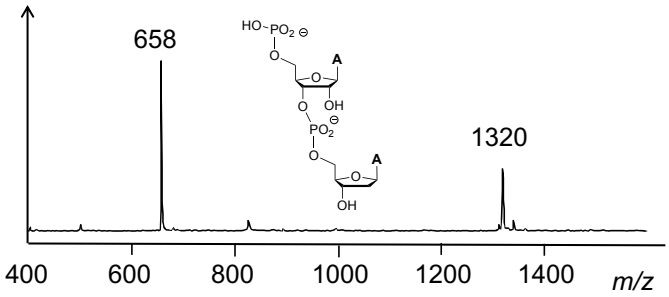

Figure S39. MALDI-TOF mass spectrum of chimeric dinucleotide 5'-pApdA. MALDI-TOF MS, calculated for $C_{20}H_{25}N_{10}O_{12}P_2$, $[M-H]^-$: 659, found: 658.

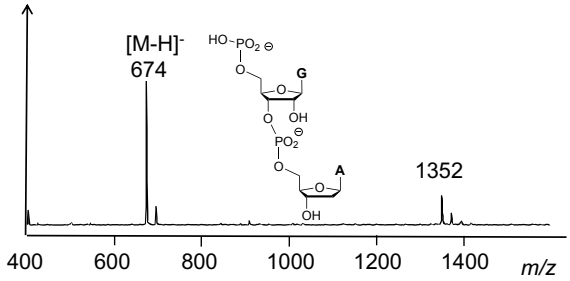

Figure S40. MALDI-TOF mass spectrum of chimeric dinucleotide 5'-pGpdA. MALDI-TOF MS, calculated for $C_{20}H_{25}N_{10}O_{13}P_2$, $[M-H]^-$: 675, found: 674.

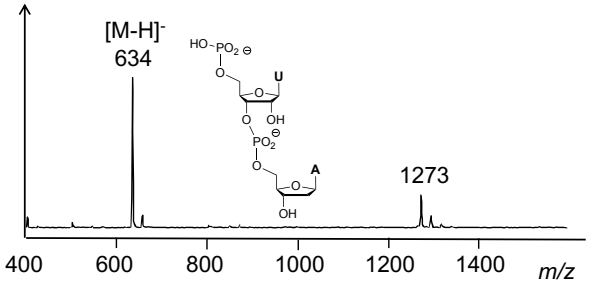

Figure S41. MALDI-TOF mass spectrum of chimeric dinucleotide 5'-pUpdA. MALDI-TOF MS, calculated for $C_{19}H_{24}N_7O_{14}P_2$, $[M-H]^-$: 636, found: 634.

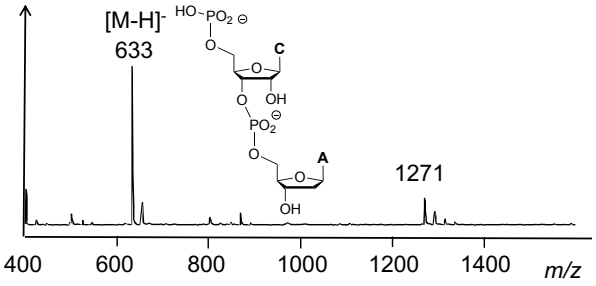

Figure S42. MALDI-TOF mass spectrum of chimeric dinucleotide 5'-pCpdA. MALDI-TOF MS, calculated for $C_{19}H_{26}N_8O_{13}P_2$, $[M-H]^-$: 635, found: 633.

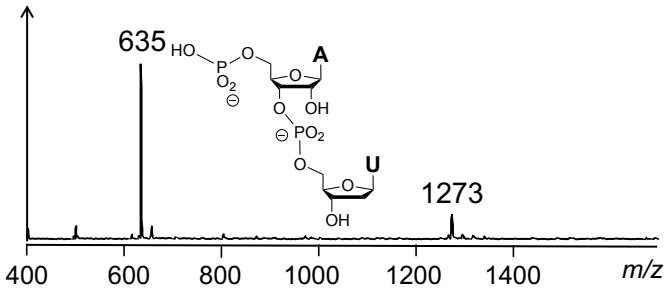

Figure S43. MALDI-TOF mass spectrum of chimeric dinucleotide 5'-pApdU.

MALDI-TOF MS, calculated for $C_{19}H_{24}N_7O_{14}P_2$, $[M-H]^-$: 636, found: 635.

6. References

1. T. Yasuda and Y. Inoue, *The Journal of Biochemistry*, 1983, **94**, 1475-1481.
2. G. M. Tener and H. G. Khorana, *Journal of the American Chemical Society*, 1955, **77**, 5349-5351.
3. R. C. Spitale, P. Crisalli, R. A. Flynn, E. A. Torre, E. T. Kool and H. Y. Chang, *Nat Chem Biol*, 2013, **9**, 18-20.
4. J. L. McGinnis, J. A. Dunkle, J. H. Cate and K. M. Weeks, *J Am Chem Soc*, 2012, **134**, 6617-6624.
5. T. H. Lowry and K. S. Richardson, *Mechanism and Theory in Organic Chemistry*, Harper & Row, 1987.
6. H. A. Staab and A. Mannschreck, *Chemische Berichte*, 1962, **95**, 1284-1297.
7. M. M. Werber and Y. Shalitin, *Bioorg. Chem.*, 1973, **2**, 221-234.